Electrofreezing of the phase-change material $CaCl_2 \cdot 6H_2O$ and its impact on supercooling and the nucleation time

Inge Magdalena Sutjahja[1], Annisa Rahman[1], Risky Afandi Putri[1], Ahmad Swandi[1], Radhiah Anggraini[1], Surjani Wonorahardjo[2], Daniel Kurnia[1] and Surjamanto Wonorahardjo[3]

[1]Department of Physics, Faculty of Mathematics and Natural Sciences, Institut Teknologi Bandung, Jl. Ganesha No. 10, Bandung 40132, Indonesia
[2]Department of Chemistry, Faculty of Mathematics and Natural Sciences, Universitas Negeri Malang, Jl. Semarang No.5, Malang, Jawa Timur 65145, Indonesia
[3]Department of Architecture, School of Architecture, Planning and Policy Development, Institut Teknologi Bandung, Jl. Ganesha No. 10, Bandung 40132, Indonesia

Abstract

This paper reports electrofreezing experiments on the inorganic phase-change material (PCM) $CaCl_2 \cdot 6H_2O$ by using an insulated copper electrode that is commonly sold in the market. The effect of the applied voltage or electric field to the nucleation process is measured by the nucleation temperature, freezing temperature, supercooling degree, induction time, time for supercooling, and time for crystallisation. It is found that, compared to the zero field, the freezing temperature remains nearly constant while the nucleation temperature increases with increasing applied field, leading to a reduction in the supercooling degree. The decrease in the supercooling degree is approximately 6 K for an applied voltage of V = 5.0 kV or $E = 10^7$ V m^{-1}. With the increase in the applied field the induction time decreased considerably along with reduction of the measured data spread as compared to the no-voltage case, while the crystallisation time for the phase transformation prolonged. The overall phenomena are analysed in terms of modification of the Gibbs free energy for crystallisation owing to the applied field, with the mechanism involving bubble generation and formation of a copper-chloride complex.

Keywords: salt hydrate, electric field, nucleation temperature; supercooling degree; induction time; thermal energy storage

Available on-line at the Journal web address: http://www.ache.org.rs/HI/

SCIENTIFIC PAPER

UDK: 536.421.48: 549.755

Hem. Ind. **73 (6)** 363-374 (2019)

1. INTRODUCTION

A phase-change material (PCM) is a material that can store sensible and latent thermal energies, with a large enough absorption capacity and heat release around its phase-transition (melting) temperature through a phase-transition process (solid–liquid and vice versa) without significant temperature changes [1-3]. This behaviour makes the heat absorption/release efficiency of a PCM much higher compared to the sensible thermal energy storage system that works based on the changes in material temperature. One application of PCMs is in a passive space air-conditioning system to achieve thermal comfort of occupants to save electrical energy for the use of air-conditioning system [4]. For this application in tropical countries such as Indonesia, $CaCl_2 \cdot 6H_2O$ (calcium chloride hexahydrate) with thermal characteristics of the melting temperature $T_m \cong 29$ °C, heat of fusion $h_f \cong 180$ kJ kg^{-1} [5-6], solid thermal conductivity $\kappa_s = 1.09$ W m^{-1} K^{-1}, and the liquid thermal conductivity $\kappa_l = 0.54$ W m^{-1} K^{-1} [7-9], is a suitable inorganic PCM [10]. Regarding the latent heat release process in the solidification process, the main problem with $CaCl_2 \cdot 6H_2O$ or common salt hydrates is a relatively large supercooling, which can reduce material performance or efficiency as a thermal energy storage system [11].

Corresponding author: Inge Magdalena Sutjahja, Department of Physics, FMIPA, ITB, Indonesia; Tel.+62-22-2512672 and Fax +62-22-2512672
E-mail: inge@fi.itb.ac.id
Paper received: 03 August 2019
Paper accepted: 09 December 2019
https://doi.org/10.2298/HEMIND190803034S

CC BY NC ND

A common way to initiate the solidification process and reduce the supercooling of PCMs, and in particular, a salt hydrate, from the solution is by seeding or adding an appropriate nucleating agent, usually in the form of nanoparticle powders, to form a stable suspension with the salt hydrate solution [12]. Lane [13] reported that the choice of the nucleating agent is usually by trial and error, guided by intuition or experience, and by using the chemical dopants which are ready in stock and on a laboratory shelf. From the crystallographic perspective, the nucleators of $CaCl_2{\cdot}6H_2O$ are classified as isomorphic and non-isostructural nucleators [13]. In general, the nucleator can impact the change in thermophysical parameters, such as the supercooling temperature, supercooling degree, specific heat, and the latent heat enthalpy. Recently, Sutjahja et al. [14] reported the effectiveness of 1 wt% CuO to reduce the supercooling degree and further modify the thermal parameters of $CaCl_2{\cdot}6H_2O$ by graphite and CuO dopants, although logical explanations for their effectiveness apparent do not exist.

The effect of electrical energy on the behaviour of supercooled fluids has been studied since two decades ago [15-16] and is commonly called electrofreezing or electronucleation; see [17-19] for the review and references therein. In most of the past experiments water droplets were mainly exposed to high-voltage electric fields, with the success expressed by higher nucleation temperatures, reduction in the supercooling degree, lowering the induction times, and increased nucleation probability. Recently, the effectiveness of electrofreezing has also been reported for some other materials, such as erythritol polyalcohol [20], tetra-n-butyl ammonium bromide (TBAB) clathrate hydrates [21-22], tetrahydrofuran (THF) clathrate hydrates [23-24], aqueous salt (NaCl) solutions [25], ammonium-based halide solution [26], aqueous glycine solutions [27], and lithium potassium sulphate (LKS) and lithium ammonium sulphate (LAS) [28], and food products [29]. The success of electrofreezing experiments were determined by certain factors, such as the type of the solution material, salt concentration, electrode material [21-22,30-32], surface properties of the electrode, electrode configuration [30-34], static (DC) or a fluctuating (AC) electric field [19,32,34-36], magnitude of the voltage or electric field [37-42], temperature at the applied field [21, 25], and duration of application of the electric field [21]. Although it is commonly observed that an increase in the electric field affects reduction in the supercooling degree, despite the variations in the experimental setups and procedures across these studies, the compiled data from many experimental results show that the magnitude of the supercooling degree is strongly dependent on the field and tends to increase by increasing the applied field [17].

The electrofreezing phenomenon is based on the impact of a strong electric field to induce crystallisation of a supercooled liquid. From the thermodynamics perspective, the process of crystallisation is initiated by the formation of nuclei and is closely related to the change in Gibbs free energy, with two main contributions from the surface free energy (ΔG_s) and volume free energy (ΔG_v). The surface free energy is the energy between the surfaceof the particle and the bulk of the particle, whereas the volume free energy is free energy between a very large and stable particle and the solute in solution [43-46]. Thus, in the absence of an applied electrostatic field, the Gibbs free energy of a spherical crystallite in solution (ΔG_0) is given by

$$\Delta G_0 = \Delta G_s + \Delta G_v = 4\pi r^2\sigma - \frac{4}{3}\pi r^3 \Delta G_v \tag{1}$$

where r is the radius of the sphere and σ is the surface free energy of the crystal fluid interface. In that formula, ΔG_v is the free-energy change of the transformation per unit volume:

$$\Delta G_v = \frac{\Delta h_f \Delta T}{T_f V_m} \tag{2}$$

where Δh_f is the molar enthalpy of fusion, V_m is the molar volume, and ΔT is the supercooling degree, as measured by the difference between the freezing temperature (T_f) and nucleation temperatures (T_N). We note that, due to different signs of the surface and volume contributions, the Gibbs free energy curve first increases with r and reaches the maximum before decreasing with the further increase of r.

In the presence of an electric field E, a new term is added to the volumetric energy, which is equal to the polarisability (P) multiplied by the electric field (E) [18]. Hence, the final equation for the Gibbs free energy of formation of a spherical nucleus under the presence of an electric field can be written as

$$\Delta G_E = 4\pi r^2\sigma - \frac{4}{3}\pi r^3\left(\Delta G_{\mathrm{v}} + PE\right) \tag{3}$$

Upon maximising the above equation, one can obtain the equation for the critical radius and critical Gibbs free energy under the influence of an electric field, as follows:

$$r_E^* = \frac{2\sigma}{\left(\Delta G_{\mathrm{v}} + PE\right)} \tag{4}$$

$$\Delta G_E^* = \frac{16\pi\sigma^3}{3\ \left(\Delta G_{\mathrm{v}} + PE\right)^2} \tag{5}$$

It is to be noted that the corresponding equations for r^* and ΔG^* obtained in the absence of an electric field do not contain the second term (*PE*) of the denominator. Thus, once the critical size for crystal formation has been reached, the Gibbs free energy decreases with the increase in the volume of the crystal [18]. Nucleation occurs spontaneously when the change in the Gibbs free energy for the system is negative.

The rate of nucleation, *J*, that represents the number of nuclei formed per unit time per unit volume can be expressed in the form of the Arrhenius equation,

$$J = A\exp\left(-\Delta G^*/kT\right) \tag{6}$$

where *A* is the pre-exponential term and *k* is the Boltzmann constant. The induction time is related to the nucleation rate as a measure of the nucleation event. Although it cannot be regarded as a fundamental property of a material because it is affected by many external factors, nor can it be relied upon to yield basic information on the process of nucleation, the formula for the induction time of true homogeneous nucleation is

$$t_{\mathrm{ind}} \propto J^{-1} = A\exp\left(-\Delta G^*/kT\right) \tag{7}$$

In experiments, the induction time is the period over which the temperature remains at the set value before a significant temperature change in the system is detected, which is due to the heat release following the nucleation [47]. From a comparison of Eqs. (4) and (5), one can see that the application of an electrostatic field leads to the modification of the critical radius and critical Gibbs free energy for the nucleation process. It is important to note that the classical nucleation theory predicts a longer time for nucleation from a solution as the complexity of molecules increases, which is due to the difficulty of arrangement in the appropriate lattice structures related to their high degree of conformational flexibility [46].

In this paper, we report electrofreezing of $CaCl_2{\cdot}6H_2O$ by using a DC electric field. The impact of the electric field on the nucleation temperature, freezing temperature, supercooling degree, induction time, and phase-transformation period were measured by variations in the magnitude and duration of the applied voltage. The results of this study are important to optimise the performance of $CaCl_2{\cdot}6H_2O$ as a thermal energy-storage system, in particular for building applications to create human comfort zones in tropical regions [10].

2. EXPERIMENTAL

For this study, we used the salt hydrate $CaCl_2{\cdot}6H_2O$ purchased from Sigma Aldrich with purity 98 %. Approximately 24 g of sample is placed in a 50-ml glass beaker with a diameter of 6 cm. The electrodes used were commonly sold copper wires of a diameter of 1.0 mm with an insulating layer. The electrode assembly was immersed completely in the sample, as shown in Figure 1, with only the tips exposed. The gap between electrodes was maintained at 0.5 mm. The DC power supply had a maximum value of 10 kV in the open state and 5 kV after the device connected to the sample.

The sensors were T-type thermocouples (with a diameter of approximately 1 mm and accuracy of ± 0.2 °C), integrated with a data logger (Applent AT4508A, Instrument Inc. from China). In order to avoid the electromagnetic interference that can affect the temperature reading of the thermocouple, we placed the temperature sensors at some

CC BY NC ND

distance from the electric field [37]. Two thermocouples were immersed in the sample and used to monitor the temperature of the sample at two different positions: at the centre of the glass beaker (T1) and at the inner circumference of the beaker (T2). The overall measurements were monitored and controlled by a PC. A water bath, provided with a controlled chamber, was set to the minimum temperature (approximately 8 °C).

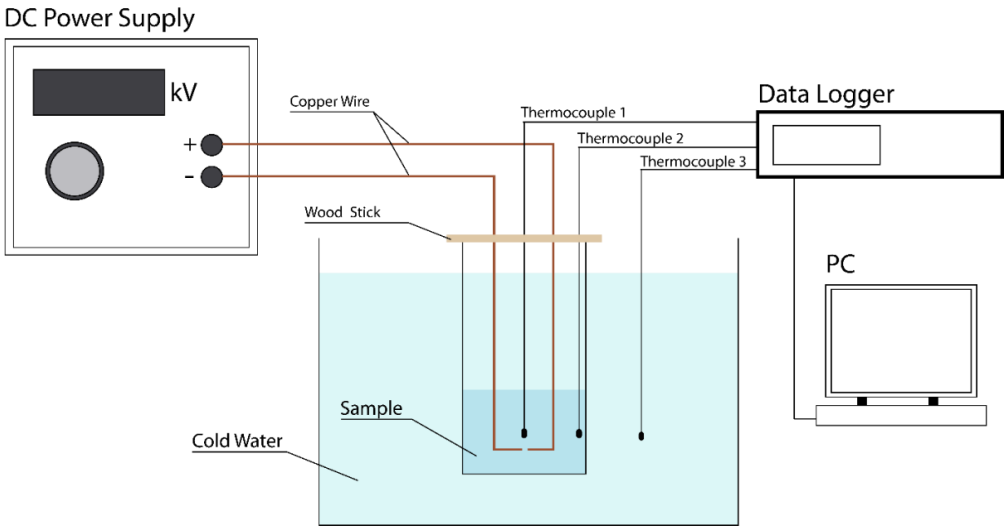

Figure 1. Scheme of the experimental set-up

Prior to measurements, the sample in the glass beaker was immersed in hot water to reach the temperature of approximately 52 °C, which is above the melting temperature of $CaCl_2 \cdot 6H_2O$ ($T_m \sim 29$ °C). After the chamber temperature was stable at a minimum temperature of approximately 8–10 °C, the sample was suddenly subjected to a cool-water environment. As the sample cooled, its temperature was measured by the temperature sensors and recorded with a data logger connected to a PC. Measurements in the zero field were repeated for three times, while measurements in the electric field were repeated five times to ensure reproducibility of the data. To reduce the impact of phase separation, a new sample was always used for each set of parameters. In all cases, the external field was applied when the temperature at the centre of the sample reached 25 °C. The case when the external field is applied at temperature 45 °C and V = 1.5 kV was also investigated.

3. RESULTS AND DISCUSSION

Figure 2 presents the typical temperature–time plot of $CaCl_2 \cdot 6H_2O$ recorded during cooling without any applied field. From this figure, starting from the high temperature of approximately 52 °C, different temperature decreases profiles recorded by the sensors located at the centre and the inner circumference of the glass beaker signify a non-uniform temperature distribution along the radial direction of the beaker owing to the large beaker diameter. The temperature decrease at the inner circumference was more rapid, as it was closer to the water environment. From each curve, the nucleation temperature (T_N) is determined as the minimum at the temperature–time curve, and it signifies the beginning of nucleation. The latent heat release following the nucleation and the crystal growth process can be seen from the steep temperature increase to reach a certain value, called the freezing temperature (T_f). The supercooling degree (ΔT) is determined as the difference between T_f and T_N. From the graph, it can be observed that the crystal growth process occurs simultaneously in all parts of the sample. However, a strong stochastic character of the nucleation process can be seen from the random time for the beginning of nucleation (t_s).

The impact of the electrostatic field on nucleation of CaCl2·6H2O is illustrated in Figure 3 for the sensor T1, along with the data obtained without the electric field from Figure 2(c), used for comparison. In this experiment, we used the voltage values of 1.5 kV, 3.0 kV, and 5.0 kV, which are the maximum values in the loading state. We note that during the experiment, the temperature values fluctuated slightly, which might be due to the electromagnetic interference [37], even though the temperature sensors were situated some distance from the electric field.

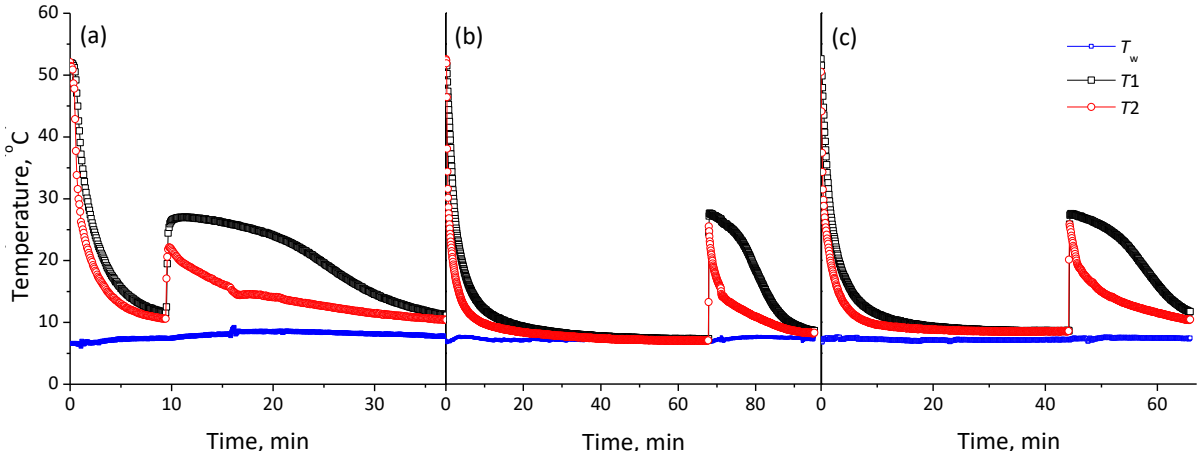

Figure 2. Temperature–time curves of $CaCl_2 \cdot 6H_2O$ in a cold-water environment at the zero field that show temperature variations for different sensor positions of T1 and T2. The water temperature is indicated by T_w. (a), (b), and (c) for the first, second, and third repetitive experiment

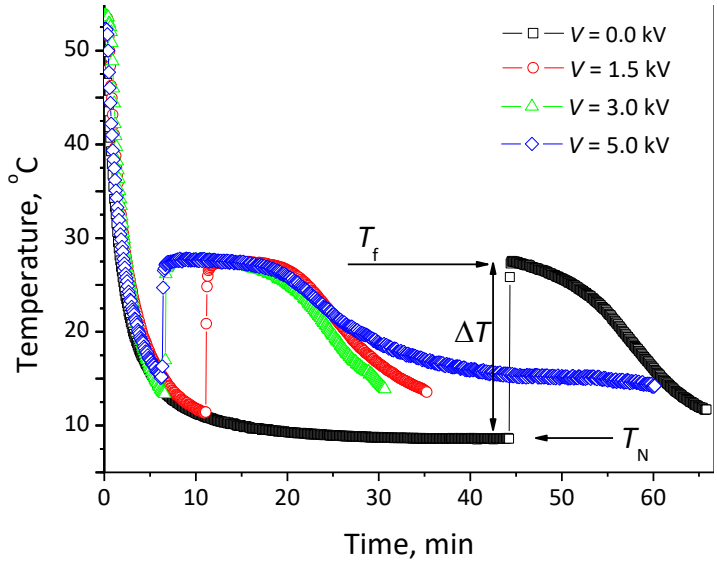

Figure 3. Nucleation of $CaCl_2 \cdot 6H_2O$ under different values of the applied electric field. In both cases, the field is applied continuously, starting at the temperature of 25 °C as measured at the centre of the sample.

Small changes (approximately 5 % of the initial value) in the voltage values might be due to the change in the current during the nucleation. The average and error values of T_N, T_f, and ΔT under different electrostatic field strengths are shown in Table 1. It can be observed that with the increase in the electric field strength, the nucleation temperature (T_N) gradually shifted towards higher values. Freezing temperatures (T_f), on the other hand, remained almost constant under different electrostatic field conditions, implying a reduction of the supercooling degree (ΔT) by the increase in the electric field strength. The increase in the nucleation temperature and reduction of the supercooling degree with the applied field was also reported for water [38], erythritol salt hydrate [20], and an aqueous salt (NaCl) solution [25].

Table 1. Experimentally determined average values of the nucleation temperature (T_N), freezing temperature (T_f), and the supercooling degree (ΔT) under different electrostatic field strengths. The error values are standard deviation values from repeated measurements

V / kV	E / V m^{-1}	$T_N \pm$ error / °C	$T_f \pm$ error / °C	$\Delta T \pm$ error / °C
0	0	9.19 ± 2.19	27.33 ± 0.37	18.13 ± 2.56
1.5	3×10^6	12.73 ± 2.16	27.20 ± 0.29	14.47 ± 2.23
3.0	6×10^6	14.17 ± 3.71	27.55 ± 0.09	13.39 ± 3.72
5.0	10×10^6	15.13 ± 1.88	27.56 ± 0.23	12.42 ± 1.79

In addition to the analysis of the impact of the electrostatic field on temperature parameters, we also analyzed time parameters, in a manner presented in the inset of Figure 4. This figure illustrates the temperature–time curve and temperature derivative-time curve during the cooling process in the zero field and in the applied field of 6×10^6 V m^{-1}.

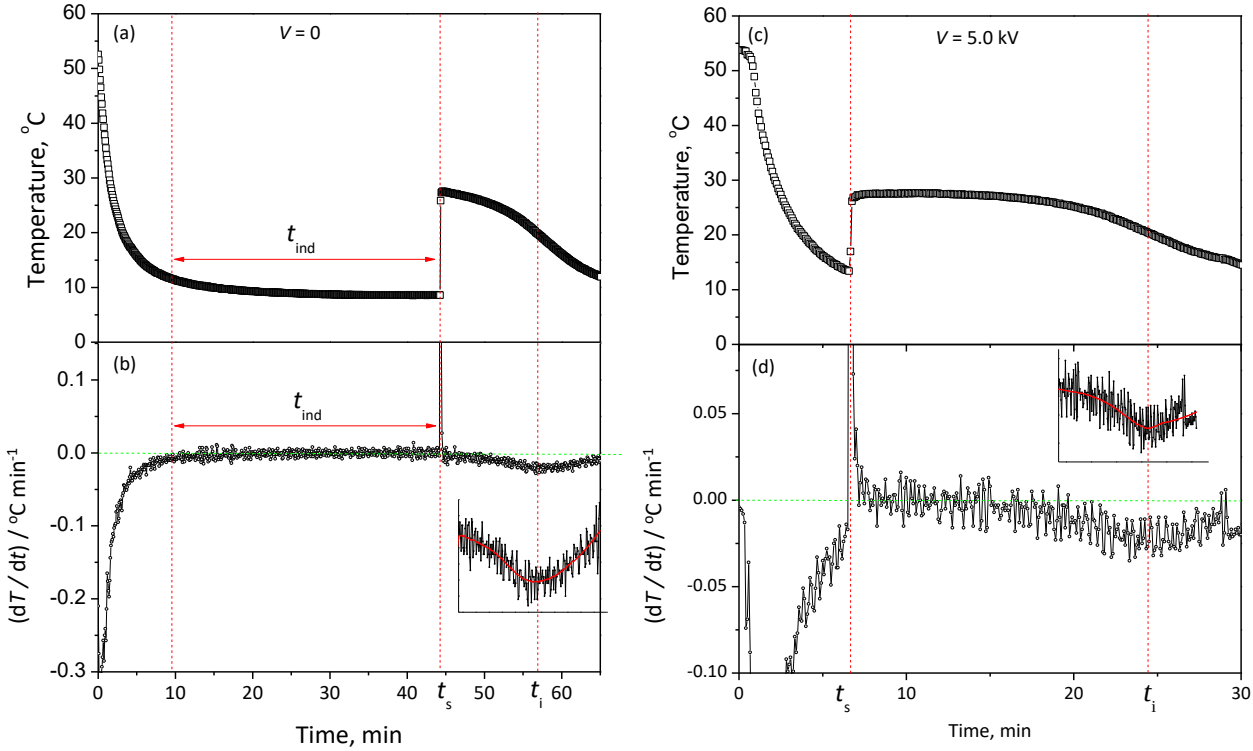

Figure 4. Temperature–time (a,c) and temperature-derivative (b,d) curves for the zero field and the applied field of E = 6×10^6 *V m*$^{-1}$ *to illustrate determination of the induction time and crystallisation time periods. The insets show the inflection time in the temperature derivative curve*

For the case of V = 0 kV, starting from the high temperature of approximately 52 °C, the cooling process leads to a temperature drop of the sample to reach a relatively constant value for a certain period. The sample temperature then increased suddenly, marking the heat released upon the hydrate nucleation at t_S. The period at a constant temperature is the induction time [47], namely the time interval required to form the very first hydrate 'seed' that is large enough for further spontaneous growth [48]. Dependence of the induction time on the applied voltage for individual experiments is presented in Figure 5(a).

From this figure, it can be seen that the induction time was lowered considerably in the presence of the electric field as compared to the no-voltage case. However, the spread in measured induction time values is significant, in particular for the case of zero voltage. The spread in induction times was reduced by the applied voltage. Similar phenomena were reported by Carpenters [23], who studied the electronucleation of tetrahydrofuran (THF) hydrates.

Unlike the sensor at the circumference of the glass beaker, a closer look at the temperature-derivative curve for the sensor at the centre revealed a dip or the inflection point (inset at Fig. 4(c,d)), signifying the overall phase transformation of the sample to the solid phase or the end of the latent heat release period. Appearance of the inflection point is due to the fact that the temperature stays constant or decreases gradually over the latent heat release but decreases exponentially in the cooling process during the sensible heat release [49]. The time and temperature positions at the dip are termed t_i and T_i, respectively. The crystallization period (t_c) signifying the overall phase transformation is determined as the difference between t_i and t_s. The results of the crystallization period t_c dependence on the voltage values are depicted in Figure 5(b). From this figure, it can be observed that t_c tended to become longer with increasing the applied field, similarly to the reports for water by Wei *et al.* [37] and Orlowska *et al.* [38]. For various parameters of the electric field, the obtained inflection temperature is approximately 21 °C with error values of approximately 1 %.

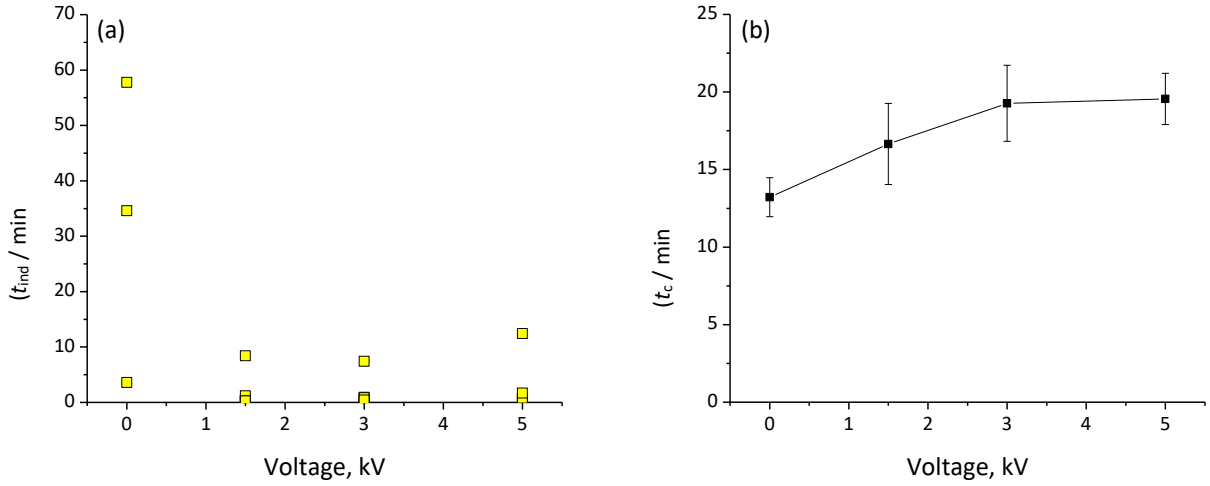

Figure 5. Experimentally determined: (a) individual induction times (t_{ind}), and (b) average and error values of the crystallization period (t_c) for different applied voltage values

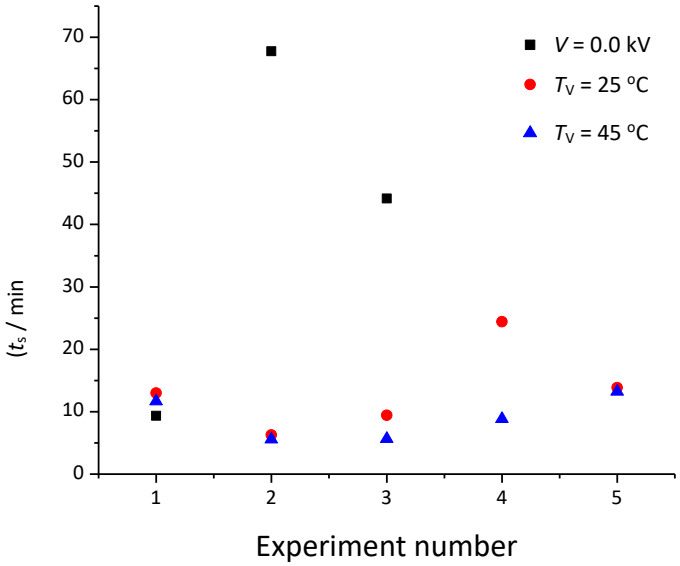

Figure 6. Supercooling times (t_s) in the individual experiments at the zero applied field and at the applied field of V = 1.5 kV at T_V = 25 °C and 45 °C

An effort to apply the electric field at a higher temperature (T_V = 45 °C) led to faster supercooling (Fig. 6) and a little higher supercooling degree. As shown in Figure 6, the shortest supercooling time is approximately 5.5 min, irrespective of the temperature, for an applied electric field of 1.5 kV and at both investigated temperatures (T_V = 25 °C and T_V = 45 °C), as compared to the longest time of approximately 67 min measured without any applied electric field. Overall, the average supercooling time in the applied electric field is approximately 10 min, with relatively small error values as compared to that at the zero field. This suggests that the application of an electric field can suppress the inherent stochastic nature of nucleation and transform nucleation to a more deterministic phenomenon.

Recent data show that the effect of an externally applied electric field is to increase the mean temperature of nucleation, reduce the supercooling degree, subsequently shorten the induction time, and prolong the solidification time. There are many explanations for the effectiveness of electrofreezing for hydrate nucleation. From the thermodynamics perspective, the Gibbs free energy required for activation is lowered with the application of an electric field energy, to yield a more favourable condition for nucleation. In the case of water droplets, Carpenter and Bahadur [23] have succeeded in distinguishing the roles of the electric field and electric current on electronucleation: controlling

CC BY NC ND

the electric field resulted in a significant increase in the nucleation temperature, up to a certain value. In the absence of the electric current flow, the electrofreezing mechanism can be attributed to the reduced nucleation activation energy upon application of an electric field. The electric current flow triggered heterogeneous electrofreezing and indicated a higher nucleation temperature. We note that the effect of adding the electrical energy in this electronucleation method is similar to adding the mechanical energy by means of mechanical treatment or by ultrasonic waves [50]. In the case of $CaCl_2{\cdot}6H_2O$, the increase in mechanical energy by mechanical treatment led to a decrease in the supercooling degree [50]. The results of the use of ultrasound irradiation in $CaCl_2{\cdot}6H_2O$ are not as clear and meaningful as water or salt [51-52], although they show similar bubble formation.

Recently, an intensive study carried out by Shahriari *et al.* [24] clearly indicated two distinct interfacial mechanisms that influenced the nucleation kinetics, namely, the electrolytic bubble formation from hydrolysis reactions and electrochemical formation of a metal ion complex-based coordination compounds. From our experimental observations, the bubble generation occurs from the negative pole of the electrode (cathode) and becomes more pronounced with increasing the applied field. These bubbles can act as nucleation sites [23–24, 32] that provide more favourable conditions for the nucleation process. In the positive pole of the electrode (anode), a chemical reaction occurs that transforms copper into Cu^{2+} ions. These ions then coalesce with Cl^- ions from the melted $CaCl_2{\cdot}6H_2O$ to form ion-complex compounds of tetrachlorocopper(II), $(CuCl_4)^{2-}$. In the water environment, these tetrahedral yellow-green $(CuCl_4)^{2-}$ ions are immediately changed to octahedral blue hexaaquacopper(II) ions, $[Cu(H_2O)_6]^{2+}$ [53], as can be seen by discoloration of the solution (greenish or bluish) after some repetitive experiments and with the change in the electric field magnitude. The bluish-coloured solution is clearly seen in the highest electric field used of 10^7 V m^{-1}. Formation of $[Cu(H_2O)_6]^{2+}$ is proven by the change in the solution colour from blue to yellow when hydrochloric acid (HCl) was added, according to the following formula [54]:

$$[Cu(H_2O)_6]^{2+} + 4\ Cl^- \rightarrow (CuCl_4)^{2-} + 6\ H_2O$$

The effectiveness of these bubble-based mechanistic effects and electrochemistry-based mechanisms have resulted in substantial acceleration of the nucleation kinetics of $CaCl_2{\cdot}6H_2O$, as shown by a very short induction time compared to that at zero field. Regarding the longer crystallisation or solidification time with the increase in the electric field, Orlowska [38] argued that it is related to the large amount of refrigeration energy stored: due to the decrease in the nucleation time, a large amount of heat that must be removed during the phase transition will result in a longer solidification time. We note, that although the effectiveness of copper electrodes has been reported for electrofreezing of other materials [21–22, 30], it is important to question whether potential of this electrode for $CaCl_2{\cdot}6H_2O$ is related to the effectiveness of copper oxide as a nucleating agent [14].

Application of PCMs as a passive air-conditioning system is commonly undertaken in two ways, both of which are integrated into building systems, including exterior walls [55] and ceilings [56], or as additional equipment separate from the building [57-58]. All methods, however, should be analysed from techno-economic and environmental impact perspectives. Integration of PCMs in building systems is generally undertaken to increase the heat capacity of the building and optimise time management for absorbing and releasing heat. Integration of a PCM in brick walls and concrete has a good effect on indoor air temperature [59-61]. However, integration of PCM in exterior walls has another effect that has not been widely discussed, namely, heat emission to the exterior environment, leading to the phenomenon generally known as the urban heat island [62], and environmental problems in recycling and treatment of the materials after use [57].

A passive air-conditioning device developed recently by Wonorahardjo *et al.* [58] is a heat exchange device that regulates day and night room temperatures. An organic coconut oil PCM (T_m = 23-26 °C) is used to absorb heat during the day and release it at night where the daily temperature ranges from 18 to 28 °C. In the tropics, where a higher temperature range is experienced, for example 25–32 °C, a PCM with a higher melting point is needed, such as $CaCl_2{\cdot}6H_2O$ ($T_m \cong 29$ °C). However, optimization of the use of a PCM requires special economic and practical techniques, such as electrofreezing, to help the process of solidification, using the capacity for supercooling of up to 18 °C.

The use of artificial air-conditioning systems for buildings in the tropics requires a very large amount of electricity, accounting for 60% of the total building energy consumption [63]. In calculating the environmental and economic

burden, these costs do not include the costs of compensation for environmental damage and its mitigation [64]. In addition, negative environmental effects, including an increase in urban air temperature or an urban heat island, generate extremely bad economic impacts, including decreased human labour productivity and micro-climate disasters, such as hurricanes, that are difficult to quantify [64]. Thus, economically, the use of thermal energy storage (TES)-based air-conditioning systems has a double impact, namely, reduction in electricity consumption for artificial air-conditioning, which has a direct effect on economy, and reduction in the cost of mitigating environmental damage, which is an indirect effect but has wide and long-lasting impacts [64]. In the context of energy poverty [65], people with low income [66] cannot provide the optimal comfort level for their house, and therefore, their productivity and life quality are very low. Globally, poverty is the main issue included in the Sustainable Development Goals (SDGs) [67], while energy waste from technologies that are not economically appropriate cannot yet be replaced. Therefore, the low-energy smart–passive technology of electro freezing is very strategic and appropriate for solving global issues.

4. CONCLUSION

We have described electrofreezing of $CaCl_2{\cdot}6H_2O$ with commonly used insulated copper electrodes. The obtained data show that the effect of the externally applied electric fields is to increase the mean temperature of nucleation and reduce the supercooling degree, resulting in a shorter induction time and longer crystallisation time. The overall phenomena are in agreement with previous experiments on water and salt hydrates. The decrease in the supercooling degree with the increase in the electric field value is related to the increase in electric energy, leading a reduction in the critical Gibbs free energy and decrease in the critical radius of the nuclei. The acceleration in nucleation kinetics of $CaCl_2{\cdot}6H_2O$ is due to bubble generation, which acts as a nucleation site, and copper-ion complexes of $(CuCl_4)^{2-}$ that immediately transform to $[Cu(H_2O)_6]^{2+}$, which is observed from the change in the solution colour after repetitive measurements and with the change in the electric field magnitude. Overall, the application of the electric field can suppress the inherent stochastic nature of nucleation and transform nucleation into a more deterministic phenomenon. The purpose of $CaCl_2{\cdot}6H_2O$ electrofreezing is in possible applications in passive air-conditioning devices is to optimize its performance as a material for latent thermal energy storage, and this method is very promising from the viewpoint of techno-economic and environmental impacts.

5. NOMENCLATURE

T_f	freezing temperature, °C
T_N	nucleation temperature, °C
ΔT	supercooling degree, °C
T_w	water's temperature, °C
T_i	inflection temperature, °C
T_V	temperature at applied electric field, °C
t_{ind}	induction time, min
t_s	supercooling/nucleation time, min
t_c	crystallization period, min
t_i	inflection time, min

Acknowledgements: This research is funded by the Desentralisasi ITB PUPT RistekDIKTI Indonesia 2018 research program under the contract number: 1170j/I1.C01/PL/2019.

REFERENCES

[1] Dinçer I, Rosen MA. *Energy Storage System and Applications*. Ontario, Canada: John Wiley & Sons, Ltd.; 2010.
[2] Bruno F, Belusko M, Liu M, Tay NHS. Using solid-liquid phase change materials (PCMs) in thermal energy storage systems. In: Cabeza LF, ed. *Advances in Thermal Energy Storage Systems, Methods and Applications*. Cambridge: Woodhead; 2015: 201-246.
[3] Fleischer AS. *Thermal Energy Storage Using Phase Change Materials Fundamentals and Applications*. Berlin: Springer; 2015.
[4] Sharma A, Kar SK (Eds.). *Energy sustainability through green energy. Thermal energy storage (part IV)*. India: Springer; 2015.
[5] Sutjahja IM, Silalahi AO, Kurnia D, Wonorahardjo S. Thermophysical Parameters and Enthalpy Temperature Curve of Phase Change Material with Supercooling from T-History Data. *U.P.B. Sci Bull Series B*. 2018; 80(2): 57-70.

CC BY NC ND

[6] Hasan A, McCormack SJ, Huang MJ, Norton B. Characterization of phase change materials for thermal control of photovoltaics using differential scanning calorimetry and temperature history method. *Energy Convers Manag.* 2014; 81**:** 322-329.
[7] Mehling H, Cabeza L. *Heat and Cold Storage with PCM*. Berlin: Springer; 2008.
[8] Tyagi VV, Kaushik SC, Pandey AK, Tyagi SK. Experimental study of supercooling and PH behavior of a typical phase change material for thermal energy storage. *Indian Journal of Pure and Applied Physics.* 2011; 49: 117-125.
[9] Nikolić R, Tripković J. Measurements of thermal conductivities of some low melting materials in a concentric cylinder apparatus. *Appl Phys A.* 1987; 44: 293-297.
[10] Zhang Y, Zhou G, Lin K, Zhang Q, Di H. Application of latent heat thermal energy storage in buildings: State-of-the-art and outlook. *Build Environ.* 2007; 42: 2197-209.
[11] Sandnes B, Rekstad J. Supercooling salt hydrates: stored enthalpy as a function of temperature. Sol Energy. 2006; 80: 616-625.
[12] Beaupere N, Soupremanien U, Zalewski L. Nucleation triggering methods in supercooled phase change materials (PCM), a review. *Thermochim Acta.* 2018; 670: 184-201.
[13] Lane GA. Phase change materials for energy storage nucleation to prevent supercooling. *Sol Energy Mater Sol Cells*. 1992: 27: 135-160.
[14] Sutjahja IM, Silalahi AO, Sukmawati N, Kurnia D, Wonorahardjo S. Variation of thermophysical parameters of PCM $CaCl_2.6H_2O$ with dopant from T-history data analysis, Variation of thermophysical parameters of PCM $CaCl_2{\cdot}6H_2O$ with dopant from T-history data analysis. *Mater Res Express*. 2018; 5: 034007(1-8).
[15] Abbas MA, Lantham J. The electrofreezing of supercooled water droplets. *J Meteorol Soc Jpn*. 1969; 47(2): 65-74.
[16] Pruppacher HR. Electrofreezing of supercooled water. *Pure Appl Geophys*. 1973; 104(1): 623-634.
[17] Acharya PV, Bahadur V. Fundamental interfacial mechanisms underlying electrofreezing. *Adv Colloid Interface Sci.* 2018; 251: 26-43.
[18] Isfahan MD, Hamdami N, Xanthakis E, Le-Bail A. Review on the control of ice nucleation by ultrasound waves, electric and magnetic fields. *J Food Eng.* 2017; 195: 222-234.
[19] Jha PK, Xanthakis E, Jury V, Le-Bail A. An Overview on Magnetic Field and Electric Field Interactions with Ice Crystallisation; Application in the Case of Frozen Food. *Crystals*. 2017; 7: 299(1-20).
[20] Jankowski NR, McCluskey FP. Electrical Supercooling Mitigation in Erythritol.In: *Proceedings of the International Heat Transfer Conference IHTC14*. Washington DC, USA, 2010.
[21] Kumano H, Hirata T, Mitsuishi K, Ueno K. Experimental study on effect of electric field on hydrate nucleation in supercooled tetra-n-butyl ammonium bromide aqueous solution. *Int J Refrig*. 2012; 35: 1266-1274.
[22] Kumano H, GotoH, Toyama Y, KawakitaM. Study on TBAB hydrate nucleating activity of electrode products due to DC voltage application. *Int J Refrig.* 2018; 93: 10-17.
[23] Carpenter K, Bahadur V. Electronucleation for Rapid and Controlled Formation of Hydrates. *J Phys Chem Lett*. 2016; 7(13): 2465-2469.
[24] Shahriari A, Acharya PV, Carpenter K, Bahadur V. Metal-Foam-Based Ultrafast Electronucleation of Hydrates at Low Voltages. *Langmuir*. 2017; 33(23): 5652-5656.
[25] Muthukumar P, Lakshmi DVN. Nucleation Enhancement Studies on Aqueous Salt Solutions, *Energy Procedia*. 2017; 109: 174-180.
[26] Yurov VM, Guchenko SA, Gyngazova MS. Effect of an electric field on nucleation and growth of crystals. *IOP Conf. Ser: Mater Sci Eng*. 2016; 110: 012019(1-6).
[27] Aber JE, Arnold S, Garetz BA, Myerson AS. Strong dc Electric Field Applied to Supersaturated Aqueous Glycine Solution Induces Nucleation of the Polymorph. *Phys Rev Lett*. 2005; 94: 145503(1-4).
[28] Hernández DR, Suárez EAD, Torres ME, Sabalisck NSP. Influence of Electric Fields over the Nucleation Ratio of the Lithium – Potassium Sulphate and its Pedagogical Value. In: *II Jornadas Iberoamaricanas de Innovación Educativaen el ámbito de las TIC*. Las Palmas de Gran Canaria, 2015, pp. 167-170.
[29] Joshaqani SF, Hamdami N, Keshavarzi E, Keramat J, Isfahan MD. Evaluation of the static electric field effects on freezing parameters of some food systems, *Int J Refrig*. 2019; 99: 30-36.
[30] Hozumi T, Saito A, Okawa S, Watanabe K. Effects of electrode materials on freezing of supercooled water in electric freeze control. *Int J Refrig*. 2003; 26: 537-542.
[31] Hozumi T, Saito A, Okawa S, Eshita Y. Effects of shapes of electrodes on freezing of supercooled water in electric freeze control. *Int J Refrig.* 2005; 28: 389-395.
[32] Shichiri T, Araki Y. Nucleation mechanism of ice crystals under electrical effect. *J Cryst Growth*. 1986; 78(3): 502-508.
[33] Piucco RO, Hermes CJL, Jader CM, Barbosa Jr R. A study of frost nucleation on flat surfaces. *Exp Therm Fluid Sci*. 2008; 32: 1710-1715.
[34] Shichiri T, Nagata T. Effect of Electric currents on the nucleation of ice crystals in the melt. *J Cryst Growth*. 1981; 54: 207-210.
[35] Stan CA, Tang SK, Bishop KJ, Whitesides GM. Externally Applied Electric Fields up to $1.6{\times}10^5$ V/m Do Not Affect the Homogeneous Nucleation of Ice in Supercooled Water. *J Phys Chem B*. 2010; 115(5): 1089-1097.

[36] Yahong M, Lisheng Z, Huiyu H, Qinxue Y, Yewen Z. A micro electro-freezing chip used in the crystallization of aqueous solutions under AC electric field. In: *IEEE 10th International Conference on the Properties and Applications of Dielectric Materials (ICPADM)*. Bangalore, India, 2012, pp. 46-49.
[37] Wei S, Xiaobin X, Hong Z, Chuanxiang X. Effects of dipole polarization of water molecules on ice formation under an electrostatic field. *Cryobiology*. 2008; 56(1): 93-99.
[38] Orlowska M, Havet M, Le-Bail A. Controlled ice nucleation under high voltage DC electrostatic field conditions. *Food Res Int*. 2009; 42: 879-884.
[39] Ma Y, Zhong L, Zhang H, Xu C. Effect of Applied Electric Field on the Formation and Structure of Ice in Biomaterials during Freezing. In: *10th IEEE International Conference on Solid dielectrics (ICSD)*. Potsdam, Germany, 2010, pp. 762-765.
[40] Yang F, Shaw RA, Gurganus CW, Chong SK, Yap YK. Ice nucleation at the contact line triggered by transient electrowetting fields. *Appl Phys Lett*. 2015; 107(26): 264101.
[41] Carpenter K, Bahadur V. Electrofreezing of Water Droplets under Electrowetting Fields. *Langmuir*. 2015; 31(7): 2243-2248.
[42] Zhang X, Li X, Chen M. Role of the electric double layer in the ice nucleation of water droplets under an electric field. *Atmos Res*. 2016; 178: 150-154.
[43] Chalmers B. *Principles of Solidification*. New York: Wiley; 1964.
[44] Mullin JW. *Crystallization*. 4th ed., Woburn, MA: Reed Educational and Professional Publishing Ltd.; 2001.
[45] Maris HJ. Introduction to the physics of nucleation. *C. R. Physique*. 2006; 7: 946-958.
[46] Myerson AS. Concluding remarks. *Faraday Discuss*. 2015; 179: 543-547.
[47] Zhang JS, Lee S, Lee JW. Kinetics of methane hydrate formation from SDS solution. *Ind Eng Chem Res.* 2007; 46(19): 6353-6359.
[48] Kashchiev D, Firoozabadi A. Induction time in crystallization of gas hydrates. *J Cryst Growth*. 2003; 250: 499-515.
[49] Hong H, Kimb SK, Kim YS. Accuracy improvement of T-history method for measuring heat of fusion of various materials. *Int J Refrig*. 2004; 27: 360-366.
[50] Young SW. Mechanical Stimulus to Crystallization in Supercooled Liquids. *J Am Chem Soc*. 1911; 33: 148-162.
[51] Günther E. Sononucleation of Inorganic Phase Change Materials, Technische Universität Munchen, 2009.
[52] Palittin ID, Kurniati N, Sutjahja IM, Kurnia D. Sonocrystallization Technique to Optimizing the Crystallization Process of PCM $CaCl_2{\cdot}6H_2O$. *Adv Mater Res*. 2015; 1112: 559-562.
[53] Tanimizu M, Takahashi Y, Nomura M. Spectroscopic study on the anion exchange behaviour of Cu chloro-complexes in HCl solutions and its implication to Cu isotopic fractionation. *Geochem J*. 2007; 41: 291-295.
[54] Vogel AI. *Vogel's Textbook of Macro and Semimicro Qualitative Inorganic Analysis*. 5th ed., SvehlaG (Ed.), New York, NY: Longman Group Limited; 1979.
[55] Agyenim F, Hewitt N, Eames P, Smyth M. A review of materials, heat transfer and phase change problem formulation for latent heat thermal energy storage systems (LHTESS). *Renew Sustain Energy Rev*. 2010; 14: 615-628.
[56] StritihU, ButalaV. Experimental investigation of energy saving in buildings with PCM cold storage. *Int J Refrig.*2010; 33: 1676-1683.
[57] Wonorahardjo S, Sutjahja IM, Kurnia D, Fahmi Z, Putri WA. Potential of Thermal Energy Storage Using Coconut Oil for Air Temperature Control. *Buildings.* 2018; 8: 95(1-16).
[58] Wonorahardjo S, Sutjahja IM, Damiati SA, Kurnia D. Adjustment of indoor temperature using internal thermal massunder different tropical weather conditions, *Science and Technology for the Built Environment*, https://doi.org/10.1080/2374-4731.2019.1608126
[59] Castell A, Martorell I, Medrano M, Pe´rez G, Cabeza LF. Experimental study of using PCM in brick constructive solutions for passive cooling. *Energy Build.* 2010; 42: 534-540.
[60] Evola G, Marletta L, Sicurella F. A methodology for investigating the effectiveness of PCM wallboards for summer thermal comfort in buildings. *Build Environ.* 2013; 59: 517-527.
[61] Álvarez S, Cabeza LF, Ruiz-Pardo A, Castell A, Tenorio JA. Building integration of PCM for natural cooling of buildings, *Appl Energy*. 2013; 109: 514-522.
[62] Wonorahardjo S, Sutjahja IM, Mardiyati Y, Andoni H, Dixon T, Achsani RA, Steven S. Characterising thermal behaviour of buildings and its effect on urban heat island in tropical areas, *International Journal of Energy and Environmental Engineering*, https://doi.org/10.1007/s40095-019-00317-0
[63] Japan International Cooperation Agency (JICA). *Development of Evaluation Method on Energy Efficiency and Conservation Policy (MACC)*; Final Report; JICA: Tokyo, Japan, 2015.
[64] Wonorahardjo S, Sutjahja IM. Bangunan Gedung Hijau untuk Daerah Tropis (Teori, Konsep, dan Penerapan). ITB Press, 2018.
[65] Schuessler R. Energy Poverty Indicators: Conceptual Issues Part I: The Ten-Percent-Rule and Double Median/Mean Indicators, Discussion Paper No. 14-037.
[66] Davis A, Padley M. The Minimum Income Standard, Loughborough University (2017).
[67] UNDP, Sustainable Development Goals, https://www.undp.org/content/dam/undp/library/corporate/brochure/SDGs_Booklet_Web_En.pdf

CC BY NC ND

SAŽETAK

Zamrzavanje $CaCl_2 \cdot 6H_2O$ indukovano električnim poljem i njegov uticaj na superhlađenje i vreme nukleacije

Inge Magdalena Sutjahja[1], Annisa Rahman[1], Risky Afandi Putri[1], Ahmad Swandi[1], Radhiah Anggraini[1], Surjani Wonorahardjo[2], Daniel Kurnia[1] i Surjamanto Wonorahardjo[3]

[1]*Department of Physics, Faculty of Mathematics and Natural Sciences, Institut Teknologi Bandung, Jl. Ganesha No. 10, Bandung 40132, Indonesia*
[2]*Department of Chemistry, Faculty of Mathematics and Natural Sciences, Universitas Negeri Malang, Jl. Semarang No.5, Malang, Jawa Timur 65145, Indonesia*
[3]*Department of Architecture, School of Architecture, Planning and Policy Development, Institut Teknologi Bandung, Jl. Ganesha No. 10, Bandung 40132, Indonesia*

(Naučni rad)

U ovom radu opisan je proces zamrzavanja neorganskog materijala koji menja agregatno stanje (Phase change material-PCM), $CaCl_2 \cdot 6H_2O$, pomoću izolovane bakarne elektrode koja je komercijalno dostupna na tržištu. Uticaj primenjenog napona ili električnog polja na proces nukleacije određen je merenjem temperature nukleacije, temperature smrzavanja, stepenom superhlađenja, vremenom indukcije, vremenom potrebnim za superhlađenje i vremenom kristalizacije. Pokazano je da u poređenju sa nultim poljem, temperatura smrzavanja ostaje gotovo constantna dok se temperatura nukleacije povećava sa porastom jačine primenjenog električnog polja, što dovodi do smanjenja stepena superhlađenja. Pad stepena superhlađenja je približno 6 K za primenjeni napon V = 5,0 kV ili $E = 10^7$ V m^{-1}. Sa porastom primenjenog električnog polja vreme indukcije se znatno smanjivalo, zajedno sa smanjenjem izmerenog širenja podataka u odnosu na slučaj bez napona, dok se vreme kristalizacije za faznu transformaciju produžilo. Opisani fenomeni su analizirani u smislu promene Gibbsove slobodne energije za kristalizaciju zahvaljujući primenjenom električnom polju, a mehanizam uključuje stvaranje mehurića i formiranje bakar-hlorid kompleksa.

Ključne reči: hidrat soli, električno polje, temperatura nukleacije; stepen super hlađenja; vreme indukcije; skladištenje toplotne energije